Journal of Genetics (2022)101:44
https://doi.org/10.1007/s12041-022-01381-y

RESEARCH ARTICLE

Functional analysis of HADH c.99C>G shows that the variant causes the proliferation of pancreatic islets and leu-sensitive hyperinsulinaemia

WU LONG[1], YUE-BING WANG[2], PENG-FEI QU[1,3], LIN MA[2], SI-JIE WEI[1], YAN-MEI XI[2], JIN-LIANG DU[1], XUE TANG[2], KAI LIU[1], YU-HUA LI[1] and PU-PING LEI[1]*

[1]*Department of Forensic Medicine, Kunming Medical University, Kunming, Yunnan Province 650500, People's Republic of China*
[2]*Institute for Endemic Disease Control and Prevention, Dali, Yunnan Province 671000, People's Republic of China*
[3]*Peking University School of Basic Medical Sciences, Beijing 100191, People's Republic of China*
*For correspondence. E-mail: puping.jacky@qq.com.

Received 20 April 2022; revised 4 July 2022; accepted 7 July 2022

Abstract. A novel missense variant (NM_005327.7: c.99C>G, p.Ile33Met) was discovered in 3-hydroxyacyl-CoA dehydrogenase (HADH), which is involved in congenital hyperinsulinism (CHI). This variant may be damaging or deleterious, as assessed using protein prediction software. This study aimed at the impact of this variant on islets and if it caused the leu-sensitive insulin secretion. The adeno-associated virus containing the HADH missense variant (p.Ile33Met), wild-type (WT) HADH or empty vector (EV) was constructed, and the rats were infected with it. Three weeks after the transfection, 15 rats were dissected to observe the effect of the variant on the islet tissue. Then we treated the remaining rats with leucine or sodium carboxymethyl cellulose (CMC-Na) by gavage and drew blood from the rat tail vein to detect the variations in blood glucose, serum insulin and serum glucagon. Further, we dissected the rats to observe the fluctuation of insulin and glucagon contents in pancreatic islets under the combined action of leucine and p.Ile33Met. Insulin and glucagon were observed in the islet tissue under an inverted fluorescence microscope, serum insulin and glucagon were detected by ELISA, and the blood glucose value was determined using a Roche glucometer. The positive area and average gray value of islet fluorescence pictures were analysed using the software Image J (USA). Rats expressing p.Ile33Met showed significantly higher insulin and glucagon content, as well as the islet area, compared to WT and EV rats. Moreover, after intragastric administration of leucine, the serum insulin content of the variant rats increased but the blood sugar level decreased significantly. Meanwhile, there was an appreciable decrease in the insulin content in rat pancreatic islet tissues. Our results suggest that the variant NM_005327.7: c.99C>G promotes the proliferation of pancreatic islets, enhances the secretion of insulin, and induces leu-sensitive hyperinsulinaemia.

Keywords. *HADH* gene; missense variant; proliferation of pancreatic islets; leu-sensitive hyperinsulinaemia.

Introduction

The 3-hydroxyacyl-CoA dehydrogenase (HADH), located at 4q25, is a member of the 3-hydroxyacyl-CoA dehydrogenase gene family with eight exons (Vredendaal *et al*. 1996, 1998). The enzyme short-chain L-3-hydroxyacyl-CoA dehydrogenase (SCHAD), encoded by HADH, is expressed in several tissues, particularly the pancreas, and plays a vital role in causing congenital hyperinsulinism (CHI), which is a heterogeneous and complex biochemical disorder characterized by unregulated insulin release and secondary hyperinsulinaemic hypoglycaemia (HH) (Agren *et al*. 1977; Galcheva *et al*. 2019). CHI typically occurs in neonates, although it can also be seen in infancy, childhood, or even adulthood (Ajala *et al*. 2016; Gutgold *et al*. 2017), and results in variable clinical phenotypes ranging from an absence of symptoms to syncope, coma, and even death (Suh *et al*. 2007; Kostopoulou and Shah 2019; Okada *et al*. 2020).

Currently, at least 14 genes (*ABCC8*, *KCNJ11*, *GLUD1*, *GCK*, *HADH*, *HK1*, *CACNA1D*, *FOXA2*, *UCP2*, *SLC16A1*, *HNF4A*, *HNF1A*, *PMM2* and *PGM1*) are related to the

Wu Long and Yue-Bing Wang contributed equally to this work.

Published online: 14 September 2022

pathogenesis of CHI, among which the activation of GLUD1 is one of the leading causes of CHI (Flanagan *et al*. 2011; Pinney *et al*. 2013; Tegtmeyer *et al*. 2014; Cabezas *et al*. 2017). However, it has been reported that HADH could inhibit the release of insulin by an inhibitory protein–protein interaction between glutamate dehydrogenase (GDH) and SCHAD (Li *et al*. 2010; Galcheva *et al*. 2019). In other words, dysfunction of HADH may upregulate GDH and secondary CHI. Moreover, the missense pathogenic variants in the HADH gene were reported to induce protein-sensitive (especially leucine) hyperinsulinaemia, resulting in higher insulin release following protein/leucine-rich meals (Satapathy *et al*. 2016; MacMullen *et al*. 2001; Santer *et al*. 2001).

In a previous study, based on whole-exome sequencing, we detected a novel missense variant (NM_005327.7: c.99C>G) from sudden unexplained deaths (Li *et al*. 2020). In HADH, the 99th nucleotide G was changed to A, leading to the change of the amino acid from isoleucine to methionine. The variant was identified using Sanger sequencing, and its protein was predicted to be potentially damaging or deleterious, as revealed by SIFT and PolyPhen2. In that study, we also learned that all the deceased had eaten local wild mushrooms whose total amino acid content and leu content were 522.81 μmol/g and 37.96 μmol/g, respectively.

Based on the above information, we proposed that the variant NM_005327.7: c.99C>G and an amino acid-rich diet could be associated with their deaths. Hence, we employed AAV8 transfection to construct variant rat models to characterize the impact of the variant on islets and then treated them with leucine to confirm whether the variant contributed to leu-sensitive insulin secretion.

Materials and methods

Building rat models with HADH c.99C>G variant

Seventy-five SPF male SD rats weighing 180–200 g were selected. The plasma glucose concentrations of these rats ranged between 4.4 and 5.6 mmol/L. The rats were divided into three groups, EV, WT, and p.Ile33Met, with 25 rats in each group, and the virus was injected at a dose of 2 × 1012 VG/mL in the tail vein of each rat. Three weeks after the transfection, five rats from each group EV, WT, and p.Ile33Met were dissected to confirm the transfection and to observe the variations in rat islets. The AAV8 vector was synthesized by Shandong Vigenebio.

Intragastric administration in rats

According to the gavage content, the remaining three groups of rats were further grouped into the vehicle group (n = 27) and administered intragastrically with 0.5% carboxymethyl cellulose sodium solution (CMC-Na), and the vehicle+leu group (n = 33), which was administered intragastrically with the CMC-Na solution and leucine. Thus, nine rats were from the EV, WT, and p.Ile33Met groups in the vehicle group, and 11 rats were from the EV, WT, and p.Ile33Met groups in the vehicle+leu group. All rats were intragastrically administered at a dose of 2 g/kg body weight (BW).

The detection of blood glucose, serum insulin, and serum glucagon in rats

Six SPF SD rats were randomly selected from each vehicle+leu group and four from each vehicle group. Then, blood samples were taken from the tail vein of the rats at three time points (before gavage, 1 h after gavage, and 2 h after gavage). The serum was obtained by centrifugation, after which about 100 μL of the serum was taken in a fresh centrifuge tube and stored at −20°C for examination. Lab consumables for the detection of serum insulin and glucagon were provided by Shanghai Xinfan Biotechnology and Jianglai Biotechnology. During the blood collection, about 10 μL of blood was used to determine the rat blood glucose using a Roche Electronic Blood Glucose Meter.

Detection of insulin and glucagon in the pancreatic islet tissue of rats by immunofluorescence

One hour after gavage, 15 rats from the vehicle group (five each in EV, WT, and p.Ile33Met groups) and 15 rats from the vehicle+leu group (five each in EV, WT, and p.Ile33Met groups) were anesthetized using ether. After laparotomy, a piece of pancreatic tissue of 0.5 cm × 0.5 cm × 0.5 cm was quickly incised from the base of the pancreas, placed in 4% paraformaldehyde PBS solution, and stored at 4°C until further examination.

The rat pancreas was embedded in a paraffin block and sectioned into thin slices. Anti-insulin antibody (mouse) and anti-glucagon antibody (rabbit) at concentrations of 1:300 and 1:1000, respectively, were used as the primary antibody. CY3 (goat anti-mouse) and CY5 (goat anti-rabbit) at a concentration of 1:300 were used as the secondary antibody, while the nucleus was stained with DAPI. The tissue sections were observed and photographed under a fluorescence microscope, and the entire picture was scanned using a slide scanner under the conditions: DAPI UV excitation wavelength 330–380 nm, blue light; GFP excitation wavelength 465–495 nm, green light; CY3 excitation wavelength 510–560 nm, red light; CY5 excitation wavelength 510–560 nm, powder light. The software Image J (USA) was used to analyse the positive area and the average gray value of the islet fluorescence pictures.

Data analysis

All the data were presented as mean±SD. Data analysis was performed using the program SPSS statistics v. 21.0 (IBM Corporation, USA), while the software Prism software

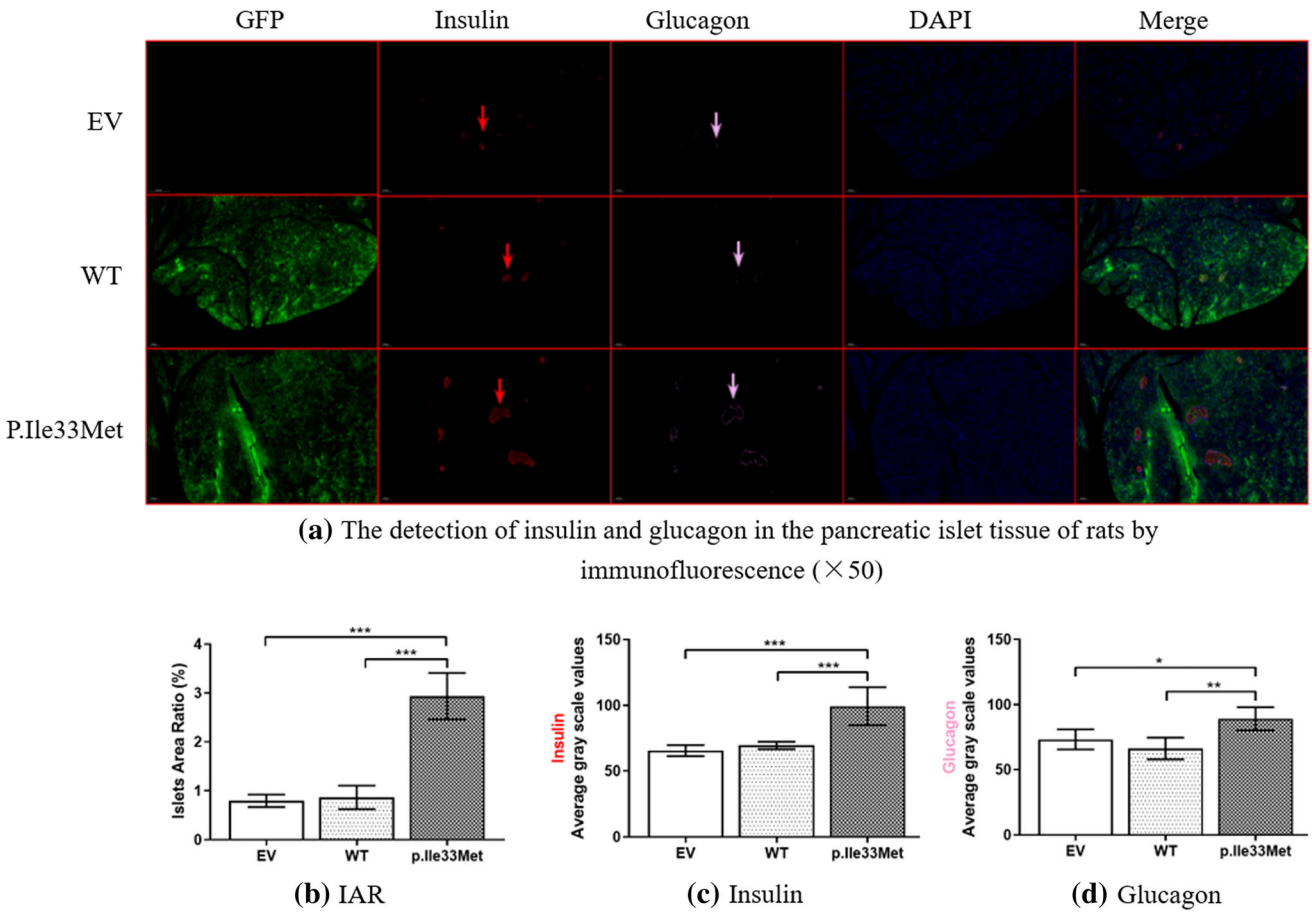

(a) The detection of insulin and glucagon in the pancreatic islet tissue of rats by immunofluorescence (×50)

(b) IAR **(c)** Insulin **(d)** Glucagon

Figure 1. Expression of NM_005327.7: c.99C>G in the rat pancreatic islets, as determined by immunofluorescence. (**a**) Rats were transfected with a GFP-tagged variant. Three weeks after transfection, the islet tissue of rats was sectioned, stained using anti-insulin (mice) or anti-glucagon (rabbit) primary antibody and fluorescent anti-mice IgG (red) or anti-rabbit IgG (pink) secondary antibody, and counterstained with DAPI (blue). The images for each group represent the fields of view from one representative rat (x50). EV, empty vector; WT, wildtype. (**b**) Islet area ratio of rat pancreatic tissue processed by Image J. Each column represents the average value for five rats. (**c, d**) Quantification of the intensity of insulin and glucagon fluorescence was determined using the software Image J after AAV8 transfection. Each column represents the average value for five rats (*$P < 0.05$; **$P < 0.01$; ***$P < 0.001$).

v.6.02 (GraphPad, La Jolla, USA) was used to draw the figures. Independent sample *t*-tests were used to compare two groups, while one-way ANOVA was used to compare three or more groups. Differences were considered statistically significant at a P value < 0.05.

Results

Three weeks after the transfection, the selected rats were dissected, their pancreas was taken, and cut into sections. The pancreas of WT rats and p.Ile33Met rats showed green fluorescence, whereas the EV rats did not, indicating the successful transfection of the target gene (figure 1a). Under a fluorescence microscope, the area with red fluorescence represents beta cells secreting insulin, the area with pink fluorescence represents alpha cells secreting glucagon, the blue fluorescence represents the cell nuclei stained with DAPI, and a combination of red and pink fluorescence can roughly show the shape of pancreatic islets.

The variant p.Ile33Met promotes the proliferation of pancreatic islets

Three weeks after the transfection, the protein expressions in the pancreas of rats of three groups differed in various aspects. The morphology of pancreatic islets in the variant rats, which appeared as irregular long strips, showed significantly increased volume compared to WT rats and those transfected with the empty vector (figure 1a). The ratio of islet area to pancreatic area (islet area ratio, IAR) of the p.Ile33Met rats was significantly higher than that of the WT rats ($P < 0.001$) and EV rats ($P < 0.001$), as revealed by the software Image J (figure 1b). The average intensity of fluorescence of pancreatic islets, both insulin and glucagon, was higher in the p.Ile33Met group than in the WT ($P < 0.001$) and EV groups ($P < 0.05$). In contrast, the WT rats and EV rats were similar in terms of the morphology, the IAR, or the fluorescence intensity of pancreatic islets (figure 1, c and d).

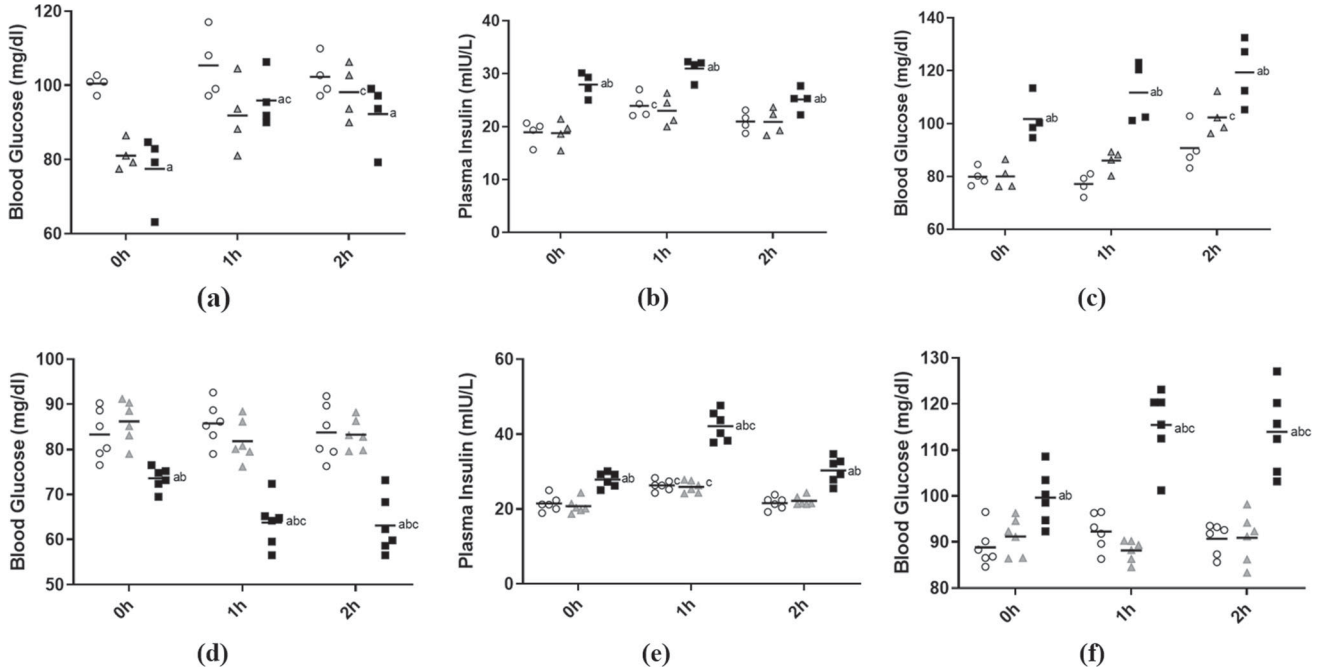

Figure 2. Three weeks after transfection, rats were administered leucine or CMC-Na solution by gavage, and the levels of blood glucose, serum insulin, and serum glucagon were determined for the specified time (before gavage, 1 h after gavage, 2 h after gavage). (**a**–**c**) Serum indices of rats after the intragastric administration of CMC-Na solution. (**d**–**f**) Serum indices of rats after the intragastric administration of leucine and CMC-Na. The circles, triangles, or squares represent the value of each replicate in EV, WT, or p.Ile33Met, respectively, and the horizontal lines denote the group average. ○represents the EV group; ▲represents the WT (Ile33) group; ■ represents the p.Ile33Met (Met33) group. **a** $P < 0.05$ compared to the EV group; **b** $P < 0.05$ compared to the WT group; **c** $P < 0.05$ compared to the same group at 0 h.

The variant p.Ile33Met induces leu-sensitive insulin secretion

Before gavage, the blood glucose levels of rats in the variant group were lower compared to rats in the other group ($P < 0.05$). After the intragastric administration of leucine at 2 g/kg BW, the differences became greater; thus, the blood glucose level of rats in the variant group dropped further ($P < 0.05$), whereas the other two groups did not show a significant change (figure 2, a and d).

In the vehicle group, the content of serum insulin and serum glucagon in the variant rats was stable before and after gavage (figure 2, b and c). In contrast, in the vehicle+leu group, the serum insulin content of variant rats showed a higher level after treatment with leucine compared to that before gavage (figure 2, e and f). In the rats transfected with the empty vector and wild-type gene, we did not observe significant changes in the blood glucose, serum insulin, or serum glucagon levels at any time point after gavage.

The intragastric administration of leucine may result in decreased insulin levels in islet of p.Ile33Met rats

After 1 h of leucine gavage, the insulin content in the pancreatic islet tissues of all the rats decreased significantly ($P < 0.05$) (figure 3, a and c), while that of glucagon decreased significantly in the EV and WT groups ($P < 0.05$) (figure 3, b and d). Moreover, after the treatment with leucine, the immunofluorescence intensity of insulin and glucagon in the variant rats was still higher than in the wild-type rats and those transfected with an empty vector ($P < 0.05$).

Discussion and conclusion

In this experiment, the rat model of NM_005327.7: c.99C>G variant was constructed and the leucine gavage intervention was to simulate the condition of the variant population following dietary intake of leucine. The experimental results indicated that NM_005327.7: c.99C>G, which we discovered in previous work (Li *et al*. 2020), can promote the proliferation of rat pancreatic islets, presented as an increase in the number of alpha cells and beta cells, upregulate the synthesis of insulin and glucagon, and exhibit dietary leucine-induced insulin secretion.

SCHAD not only participates in the β oxidation of fatty acids but also acts as a moonlighting protein that binds to GDH and inhibits its activity (Li *et al*. 2010). GDH encoded by GLUD1 catalyzes the oxidative deamination of glutamate to ammonia and α-ketoglutarate. Then, alpha-ketoglutarate enters the tricarboxylic acid cycle in beta cells to induce the release of insulin (Roy *et al*. 2019). The deficiency of HADH weakens the protein–protein inhibitory interaction of SCHAD with GDH, thereby promoting insulin secretion.

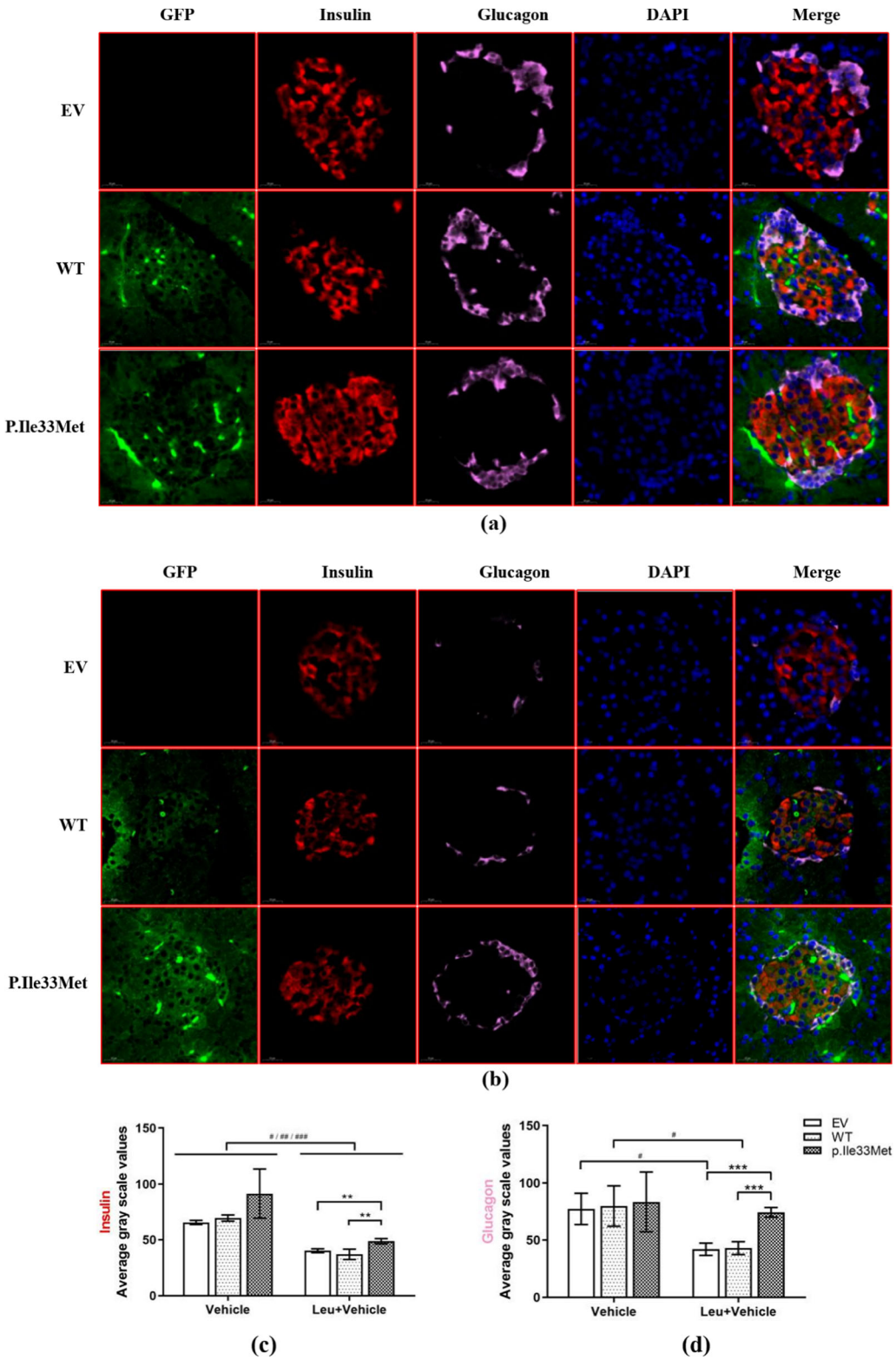

Figure 3. Immunofluorescence of the rat pancreatic islet tissue at 1 h after the intragastric administration of leucine or CMC-Na solution. (a) Immunofluorescence images of sections from the rats administered CMC-Na solution through gavage (x400). Images for each group are representative fields of view from one representative rat. (b) Immunofluorescence images of sections from the rats administered the solution containing leucine and CMC-Na through gavage (x400). Images for each group are representative fields of view from one representative rat. (c, d) Quantification of the immunofluorescence intensity of insulin or glucagon in the rat pancreas. Each column represents the average value for five rats. EV, empty vector; WT, wild type. □ represents the EV group; ■ represents the P.Ile33Met(Met33) group (*$P < 0.05$; **$P < 0.01$; ***$P < 0.001$; #$P < 0.05$; ##$P < 0.01$; ###$P < 0.001$).

Hardy *et al*. (2007) confirmed that the use of siRNA to inhibit HADH activity in pancreatic beta cells can significantly increase the level of insulin secretion. Li *et al*. (2010) observed that the fasting plasm insulin levels in HADH-knockout mice were approximately twice compared to those in normal mice. In our experiments, although the content of insulin in variant rats increased significantly, we could not conclude whether variant p.Ile33Met weakened the inhibitory effect of HADH on GDH as we could not verify the mechanism of interaction between them. Besides, due to the significantly enlarged islets, we propose that the increase in insulin secretion may be based on islet hyperplasia. However, the mechanism of islet hyperplasia in the p.Ile33Met variant should be further studied.

The release of insulin, an important regulator of metabolism, is regulated by multiple dietary factors, such as glucose, free fatty acids, and amino acids, especially branched-chain amino acids (BCCA) (van Loon *et al*. 2003; Nolan *et al*. 2006; Newsholme *et al*. 2007). BCCAs include leucine (leu), valine, and isoleucine, among which leu has the strongest activating effect on GDH (Stanley *et al*. 1998; Li *et al*. 2011). SCHAD has been demonstrated to protect against excess amino acid-induced insulin secretion (Kapoor *et al*. 2009). Consequently, once defective missense pathogenic variants of HADH are generated, a protein/leu-sensitive hyperinsulinaemia would be produced. In our experiments, the serum insulin of variant rats, at 1 h after administration of leu, increased significantly compared to the other groups, while the insulin content in pancreatic islet tissues of variant rats decreased significantly. This confirms the existence of leu-sensitive insulin release in the variant rats. Besides, it was worth noting that the serum insulin content of the mutant rats was significantly higher than that of the other two groups after the administration of leu by gavage, while the content of insulin in the tissues, although decreased, was still higher than that in the WT and EV groups, indicating that the mutant mice had a higher amount of insulin.

Hyperinsulinism caused by leucine gavage induced a significant reduction in the blood glucose levels in the variant rats, although it did not reach the clinical level of 'low blood sugar' (< 50 mg/dL) as observed in NM_005327.7: c.101G>C patients based on an amino acid load test (Snider *et al*. 2013). Variant in the same gene show different blood glucose levels, which may be related to different variant gene loci, or may be caused by the concomitant increase in glucagon in this experiment. Also, this result might help to explain the benign nature of the variant p.Ile33Met in some patients (Nykamp *et al*. 2017). Further, we dissected the rats and observed that there was still some leu as a white powder in the rat's stomach and small intestine, indicating the incomplete absorption of leucine, which may be related to the blood glucose level of the rat. The data that support the findings of this study are available from the corresponding author upon reasonable request.

In conclusion, our study demonstrated the novel variant NM_005327.7: c.99C>G can increase the size of pancreatic islets, enhance its secretory function, and manifest leu-sensitive insulin secretion. This is our preliminary finding on this variant, which may facilitate further investigation of its function and allow for the screening of genetic diseases in other family members.

Acknowledgements

This work was funded by the National Natural Science Foundation of China (81460285, 81960573), the Applied Basic Research Projects of Yunnan Province (202101AY070001-008), and the Innovation Group of Kunming Medical University (CXTD201803). All authors are grateful to the Department of Laboratory at the Animal Science and Technology Achievement Incubation Center at Kunming Medical University for technical support and thoughtful insights.

Authors' contributions

PPL and Y-BW contributed to the study design. WL, PFQ, JLD performed experiments and produced the first draft of the manuscript. LM, YMX, XT analysed the data. S-JW, KL, YHL captured pictures and image processing. P-PL and WL performed a final critical review of the manuscript. All the authors read and approved the final manuscript.

References

Agren A., Borg K., Brolin S. E., Carlman J. and Lundqvist G. 1977 Hydroxyacyl CoA dehydrogenase, an enzyme important in fat metabolism in different cell types in the islets of Langerhans. *Diabetes Metab. J.* **3**, 169–172.

Ajala O. N., Huffman D. M. and Ghobrial I. I. 2016 Glucokinase variant-a rare cause of recurrent hypoglycemia in adults: a case report and literature review. *J. Commun. Hosp. Int.* **6**, 32983.

Cabezas O. R., Flanagan S. E., Stanescu H., Garcia-Martinez E., Caswell R., Lango-Allen H. *et al*. 2017 Polycystic kidney disease with hyperinsulinemic hypoglycemia caused by a promoter variant in phosphomannomutase 2. *Am. Soc. Nephrol.* **28**, 2529–2539.

Flanagan S. E., Kapoor R. R. and Hussain K. 2011 Genetics of congenital hyperinsulinemic hypoglycemia. *Semin. Pediatr. Surg.* **20**, 13–17.

Galcheva S., Demirbilek H., Al-Khawaga S. and Hussain K. 2019 The genetic and molecular mechanisms of congenital hyperinsulinism. *Front. Endocrinol.* **10**, 111.

Gutgold A., Gross D. J., Glaser B. and Szalat A. 2017 Diagnosis of ABCC8 congenital hyperinsulinism of infancy in a 20-year-old man evaluated for factitious hypoglycemia. *J. Clin. Endocrinol. Metab.* **102**, 345–349.

Hardy O. T., Hohmeier H. E., Becker T. C., Manduchi E., Doliba N. M., Gupta R. K. *et al*. 2007 Functional genomics of the β-cell: short-chain 3-hydroxyacyl-coenzyme A dehydrogenase regulates insulin secretion independent of K+ currents. *Mol. Endocrinol.* **21**, 765–773.

Kapoor R. R., James C., Flanagan S. E., Ellard S., Eaton S. and Hussain K. 2009 3-Hydroxyacyl-coenzyme A dehydrogenase deficiency and hyperinsulinemic hypoglycemia: characterization of a novel variant and severe dietary protein sensitivity. *J. Clin. Endocrinol. Metab.* **94**, 2221–2225.

Kostopoulou E. and Shah P. 2019 Hyperinsulinaemic hypoglycaemia-an overview of a complex clinical condition. *Eur. J. Pediatr.* **178**, 1151–1160.

Li C., Chen P., Palladino A., Narayan S., Russell L. K., Sayed S. *et al*. 2010 Mechanism of hyperinsulinism in short-chain 3-hydroxyacyl-CoA dehydrogenase deficiency involves activation of glutamate dehydrogenase. *J. Biol. Chem.* **285**, 31806–31818.

Li L. J., Wang Y. B., Qu P. F., Ma L., Liu K., Yang L. *et al*. 2020 Genetic analysis of Yunnan sudden unexplained death by whole genome sequencing in Southwest of China. *J. Forensic Leg. Med.* **70**, 101896.

Li M., Li C., Allen A., Stanley C. A. and Smith T. J. 2011 The structure and allosteric regulation of glutamate dehydrogenase. *Neurochem. Int.* **59**, 445–455.

MacMullen C., Fang J., Hsu B. Y., Kelly A., de Lonlay-Debeney P., Saudubray J. M. *et al*. 2001 Hyperinsulinism/hyperammonemia syndrome in children with regulatory variants in the inhibitory guanosine triphosphate-binding domain of glutamate dehydrogenase. *J. Clin. Endocrinol. Metab.* **86**, 1782–1787.

Newsholme P., Bender K., Kiely A. and Brennan L. 2007 Amino acid metabolism, insulin secretion and diabetes. *Biochem. Soc. Trans.* **35**, 1180–1186.

Nolan C. J., Madiraju M. S., Delghingaro-Augusto V., Peyot M. L. and Prentki M. 2006 Fatty acid signaling in the beta-cell and insulin secretion. *Diabetes* **55**, 16–23.

Nykamp K., Anderson M., Powers M., Garcia J., Herrera B., Ho Y. Y. *et al*. 2017 Sherloc: a comprehensive refinement of the ACMG-AMP variant classification criteria. *Genet. Med.* **19**, 1105–1117.

Okada S., Fukunaga S., Ohta H., Furuta T., Hirano R., Motonaga T. *et al*. 2020 Cerebral insufficiency caused by diazoxide in a premature neonate with congenital hyperinsulinism. *Neuropediatrics* **51**, 211–214.

Pinney S. E., Ganapathy K., Bradfield J., Stokes D., Sasson A., Mackiewicz K. *et al*. 2013 Dominant form of congenital hyperinsulinism maps to HK1 region on 10q. *Horm. Res. Paediatr.* **80**, 18–27.

Roy K., Satapathy A. K., Houhton J., Flanagan S. E., Radha V., Mohan V. *et al*. 2019 Congenital hyperinsulinemic hypoglycemia and hyperammonemia due to pathogenic variants in GLUD1. *Indian J. Pediatr.* **86**, 1051–1053.

Santer R., Kinner M., Passarge M., Superti-Furga A., Mayatepek E., Meissner T. *et al*. 2001 Novel missense variants outside the allosteric domain of glutamate dehydrogenase are prevalent in European patients with the congenital hyperinsulinism-hyperammonemia syndrome. *Hum. Genet.* **108**, 66–71.

Satapathy A. K., Jain V., Ellard S. and Flanagan S. E. 2016 Hyperinsulinemic hypoglycemia of infancy due to novel HADH variant in two siblings. *Indian Pediatr.* **53**, 912–913.

Snider K. E., Becker S., Boyajian L., Shyng S. L., MacMullen C., Hughes N. *et al*. 2013 Genotype and phenotype correlations in 417 children with congenital hyperinsulinism. *J. Clin. Endocrinol. Metab.* **98**, E355-363.

Stanley C. A., Lieu Y. K., Hsu B. Y., Burlina A. B., Greenberg C. R., Hopwood N. J. *et al*. 1998 Hyperinsulinism and hyperammonemia in infants with regulatory variants of the glutamate dehydrogenase gene. *N. Engl. J. Med.* **338**, 1352–1357.

Suh S. W., Hamby A. M. and Swanson R. A. 2007 Hypoglycemia, brain energetics, and hypoglycemic neuronal death. *Glia* **55**, 1280–1286.

Tegtmeyer L. C., Rust S., van Scherpenzeel M., Ng B. G., Losfeld M. E., Timal S. *et al*. 2014 Multiple phenotypes in phosphoglucomutase 1 deficiency. *N. Engl. J. Med.* **370**, 533–542.

van Loon L. J., Kruijshoop M., Menheere P. P., Wagenmakers A. J., Saris W. H. and Keizer H. A. 2003 Amino acid ingestion strongly enhances insulin secretion in patients with long-term type 2 diabetes. *Diabetes Care* **26**, 625–630.

Vredendaal P. J., van den Berg I. E., Malingre H. E., Stroobants A. K., Olde W. D. and Berger R. 1996 Human short-chain L-3-hydroxyacyl-CoA dehydrogenase: cloning and characterization of the coding sequence. *Biochem. Biophys. Res. Commun.* **223**, 718–723.

Vredendaal P. J., van den Berg I. E., Stroobants A. K., van der Aee D. L., Malingre H. E. and Berger R. 1998 Structural organization of the human short-chain L-3-hydroxyacyl-CoA dehydrogenase gene. *Mamm. Genome* **9**, 763–768.

Corresponding editor: Durgadas P. Kasbekar